Development and characterisation of a Dynamic Mass Instrument (DMI) for use in microwave heating experiments.

James D. Cole[1]⋆, Simon Sheridan[1], Sungwoo Lim[2], Hannah M. Sargeant[3], Mahesh Anand[1], Andrew D. Morse[1]

[1]*School of Physical Sciences, Open University, Milton Keynes, MK7 6AA, UK*

[2]*Surrey Space Centre, University of Surrey, Guildford, GU2 7XH, UK*

[3]*Space Park Leicester, University of Leicester, Leicester, LE4 5SP, UK*

ABSTRACT

This study describes the development of an instrument known as the Dynamic Mass Instrument (DMI) for use in microwave heating experiments that will allow greater insight in to the efficacy of the technique. A commercially available load cell is used as the main mechanism of mass measurement with a load arm used to provide microwave isolation of the load cell. The DMI is capable of measuring changes in mass with a mass range of 100 g to 200 g with an accuracy of ± 0.1 g in an environment of 250 W, 2.45 GHz microwaves under a working pressure of 3 mbar. A series of calibrations and experiments have been performed to quantify and clarify the behaviour of the instrument in different environments and scenarios and to ensure the DMI meets preset requirements. The DMI will, in future work, be used in In Situ Resource Utilisation (ISRU) experiments to examine in greater detail the efficacy of using microwave heating as a water extraction technique.

Key words: ISRU – Microwave Heating – Instrumentation – Lunar Water – Space Exploration

1 INTRODUCTION

In-Situ Resource Utilisation (ISRU) has the potential to significantly reduce the mass and cost of space missions as vital resources required for missions can be gathered and processed at the in-situ and therefore do not need to be launched from the Earth's gravity well (Sanders & Larson 2013). Water ice is a highly coveted resource due to its high number of uses and crucial economic value in a cislunar economy (Metzger 2023). As a liquid, water can be used to sustain a crewed lunar base through the supply of drinking water and is a major resource for agriculture processes. If the water is electrolysed into oxygen and hydrogen, oxygen can be used for breathable atmospheres and both can be used as rocket propellant in LH2/LOX systems (Schlüter & Cowley 2020; Metzger 2023). Creating a rocket propellant infrastructure on the lunar surface could lead to a multi-billion dollar cislunar economy as lunar water derived rocket propellant could be used to launch cargo and crew off the lunar surface, refuel satellites in cislunar space, and even launch missions deeper into the Solar System (Kornuta et al. 2019; Metzger 2023). Due to the low obliquity of the Sun at the lunar poles, regions in deep craters known as Permanently Shadowed Regions (PSRs) never experience any sunlight and many exist with maximum temperatures of < 110 K allowing stable water ice to exist in these locations (Watson et al. 1961; Paige et al. 2010). Ice is believed to have been delivered to these regions through a mixture of cometary/meteorite impacts and solar wind deposition (Anand 2010; Cannon & Britt 2020). Remote sensing measurements have found particular PSRs to contain upwards of 30 wt. % ice content, while an in-situ measurement of an impact plume taken during the LCROSS mission measured an ice content of 5.6 ± 2.9 wt. % (Li et al. 2018; Colaprete et al. 2010). Microwave heating offers the possibility of high efficiency extraction of water ice from icy deposits at the lunar poles (Ethridge & Kaukler 2007; Cole et al. 2023). The ability of microwave energy to provide deep volumetric heating, overcoming the low thermal conductivity of lunar regolith, leads to quicker, more efficient heating of lunar simulants compared to conductivity dependent techniques such as solar sintering and joule heating (Taylor & Meek 2005; Lim et al. 2021, 2023). Understanding the quantity of water that can be released from cryogenic icy simulant samples in a laboratory setting using microwave heating provides much needed inputs for a demonstrator ISRU payload. Many questions remain regarding how much water can be extracted with different alterations to the samples including increased water content and different ice forms (Cole et al. 2023). The ability to measure the mass change of a heated sample in real time will allow greater constraining of the heating time, energy inputs, and sample composition requirements of an ISRU payload. The objective of this was study was to develop an instrument, known as the Dynamic Mass Instrument (DMI), that can measure the changing mass of a sample while the sample is heated in a microwave environment under vacuum conditions. In this study, a dynamic mass is a mass that changes over time and therefore requires an instrument that can measure the mass over time. Various experiments are performed to characterise the performance of the instrument. In the future, the DMI will be used in a full experimental campaign to examine the efficacy of using microwave heating to extract water from icy regolith samples.

⋆ E-mail: james.cole@open.ac.uk

Table 1. The requirements specification of the Dynamic Mass Instrument.

Req. Number	Requirement Description
1	The instrument must operate in a microwave environment of at least 250 W.
2	The instrument must record dynamic masses with an accuracy of ± 0.1 g.
3	The instrument must record dynamic masses in a sample mass range of 100 g to 200 g.
4	The instrument must include no metal or high dielectric loss materials in the microwave cavity.
5	The instrument must operate in a vacuum environment below 3 mbar based on previous experiments (Cole et al. 2023).
6	The instrument must be configured in such a way that it can be used on an existing microwave system (Described in Lim et al. (2021)).
7	The instrument must be able to handle samples with a temperature range of 100 – 400 K.

2 INSTRUMENT DESCRIPTION

During development, it was decided the DMI needed to meet a certain number of requirements shown in Table 1. The most important design criteria for the DMI was that the instrument would need to be built around an existing microwave heating unit, described in greater detail in Lim et al. (2021) and shown in Figure 1 a). This both impacted the practical design, but also meant the instrument must be compatible with microwave energy and not impact the ability of the microwave cavity to heat samples. The DMI mass accuracy and vacuum requirements of ± 0.1 g and 3 mbar respectively were taken from values in a previous study that used the same microwave system for ISRU experiments (Cole et al. 2023). The mass range was based on the mass of sample crucible (100 g) and simulant (50 g). The DMI uses a commercially available load cell with a capacity of 500 g (TALS 221) as the main mechanism of mass measurement. An excitement voltage of 4.60 V was supplied using a DC power supply (EMS Power 9888) and the signal voltage was measured in mV using a multimeter (Keithley 2000). To calculate the change in mass, the difference in two signal voltage readings is taken. A drawing of a section view of the DMI can be seen in Fig. 1 b). The load cell is kept away from the microwave source as the microwaves interfere with the electronics and aluminium alloy that makes up the load cell. The microwave cavity door has a milled cut-out in the curved wall with a width of 3.5 cm and height of 2 cm. As this height and width is smaller than the wavelength of the 2.45 GHz microwaves, a negligible amount of microwave energy can permeate through the cut-out. Through the gap, a CF63 vacuum tee fitting is attached with the load cell attached at the far end of the fitting. From here, all the electronics are wired through a flange feed-through. As the load cell is placed far from the cavity, a load arm is attached to the load cell and then fed through the cut-out into the microwave cavity. The entire arm is created from PTFE pieces and two alumina rods as seen in an internal model of the DMI system itself in Fig. 1 c). As both PTFE and alumina ceramic have low dielectric loss factors at 2.45 GHz, they absorb negligible microwave energy, and therefore make ideal construction materials for microwave heating purposes (Yaw 2012). Furthermore, PTFE can be milled to design while alumina ceramic is strong enough to support the masses placed on the load arm. The load arm has a mass of 53 g and therefore gives the load cell a different zero-offset to the sample being placed directly onto the load cell. The entire DMI is loaded onto two protruding bars with

a bearing system allowing the door to be rolled back and for samples to be loaded into the system. The DMI was built as shown in Fig. 1 d) and then calibrations were conducted to quantify the behaviour of the instrument.

3 EXPERIMENTAL DESCRIPTIONS

3.1 Calibrations

Calibration experiments were crucial to ensure accurate measurements using the DMI could be made. The calibrations allowed any unknown behaviour of the instrument to be defined and quantified before an experimental campaign could be performed. Therefore a series of calibration experiments were performed to measure certain characteristics of the instrument. They are i) creep/non-linearity ii) sensitivity iii) drift and iv) hysteresis/repeatability.

(i) An initial set of calibrations were required to define the creep and non-linearity of the instrument. Creep is a measurement of the variation in the signal voltage when the load is first placed or removed from the load cell. Creep testing was performed first to check how much time was required for an accurate and stable measurement of the signal voltage to be ascertained. This is caused by a time delay before the signal voltage is accurate due to the creep. Therefore, the signal voltage was measured for 4000 s with a 100 g calibrated mass placed on the load arm for 3000 s of that time. The remaining time was used to take zero measurements both before and after the loading to check how much zero creep was present. Non-linearity was tested by measuring the signal voltage response from calibrated masses between 100 g and 200 g. There was a focus on the 125-150 g range as this is the mass of the majority of samples that are processed in the microwave cavity (Lim et al. 2021; Cole et al. 2023). Calibrated masses were measured on an external mass balance with a resolution of ± 0.1 g. The difference between the signal voltage output and the expected output for ideal linear response was used to calculate the non-linearity.

(ii) The sensitivity of the load cell on the datasheet is quoted at 0.7 ± 0.15 mV/V. The quoted error in the sensitivity was too large for the instrument to possess the required mass resolution, therefore it was decided to calibrate the instrument and calculate the sensitivity in the mass range of our requirements (100-200 g). The sensitivity was altered resulting in different calculated mass outputs. The percentage error between the calculated mass and the measured masses of the calibrated masses was used to assess the most appropriate sensitivity.

(iii) The long term drift of the DMI while under load was measured. A calibrated mass of 100 g was placed on the load arm and then exposed to various environments. The signal voltage was measured for a long period (> 70 hours) where over regular periods, the environment was switched between atmospheric air and a 3 mbar vacuum. The change in environment was designed to check the effects of pressure and temperature on the load cell.

(iv) The hysteresis was measured by loading masses onto the load cell in increasing mass before de-loading the mass in reverse order. This was done with masses ranging from 1 g to 200 g with a second repeat. Each load was measured for 900 s before the next load was placed or removed.

3.2 Dynamic Mass Experiment

A dynamic mass experiment was designed to test how well the DMI responded to a mass that changes over time. No microwave energy
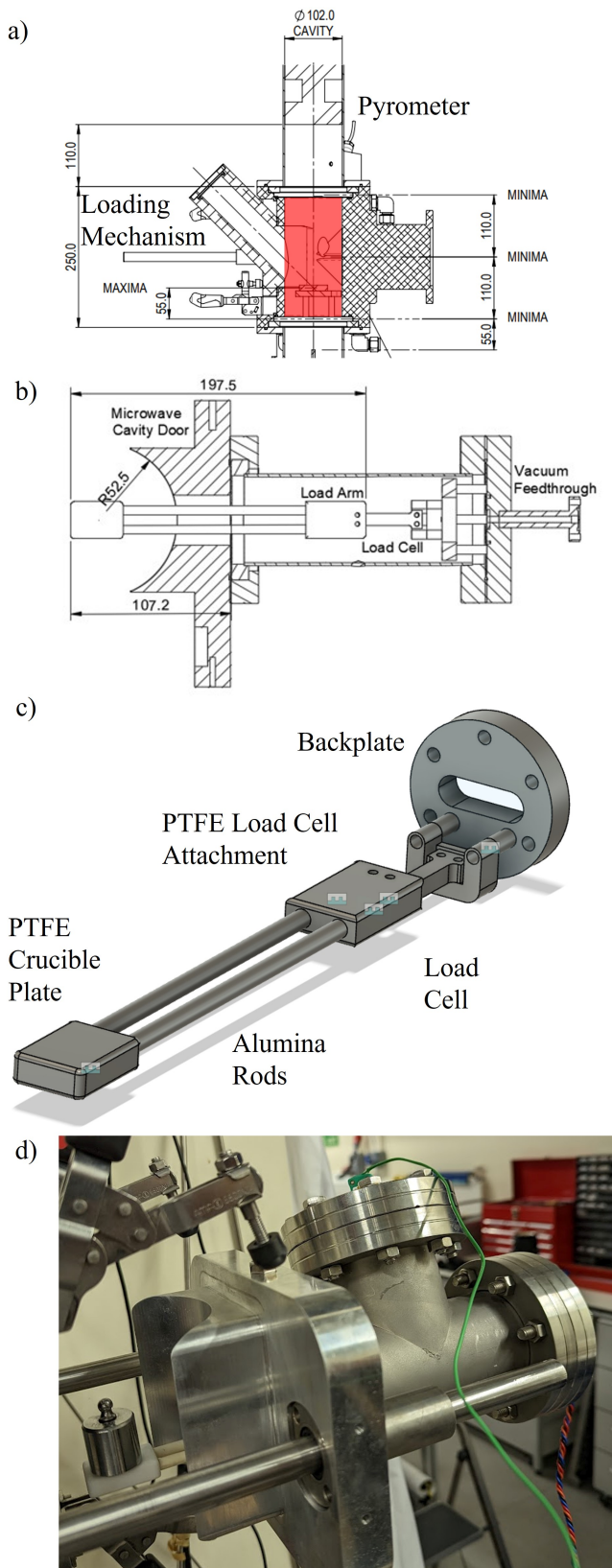
Figure 1. Diagrams of the DMI design.a) A section view of the microwave system. The red box highlights the microwave cavity. b) A section view of the DMI. The load cell is separated from the microwave cavity through the use of a small cut-out and a load arm. c) Internal CAD model of the load cell and load arm design. d) The built DMI attached to the microwave system.

was used at this point to avoid introducing excess variables. Approximately 10 g of IsoPropyl Alcohol (IPA) was placed in an alumina crucible. The total mass of the sample was measured on an external mass balance with a readout precision of $\pm$ 0.1 g. The crucible was then placed on the DMI load arm, and placed in a vacuum of 3 mbar using a scroll pump. The mass of the sample was measured using the DMI as the IPA evaporated in the vacuum conditions. After 80 minutes, the DMI was removed from the vacuum chamber and the final sample mass was measured on the external mass balance.

3.3 Microwave Environment Experiment

It was essential to test the DMI in a microwave environment to ensure that all microwave energy was isolated from the load cell and no interference was experienced in the load cell. An alumina crucible was filled with 6 g of deionised H_2O and heated using microwave energy in 3 separate heating runs at a vacuum of 3 mbar using 250 W, 2.45 GHz microwaves. The heating times were 10, 15, and 30 minutes respectively. At the end of each respective run, the DMI was removed from the microwave cavity and the sample mass was measured on the external mass balance. The sample was then placed back on the DMI and placed into the microwave cavity.

4 RESULTS

4.1 Calibrations

The results for the calibrations experiments are listed below:

(i) Fig. 2 shows the signal voltage after loading the 100 g mass. The signal voltage when the mass reading had plateaued and the signal voltage upon initial loading were compared. The difference between the two readings is 0.001 mV which is equivalent to 0.15 g. While this represents a positive creep higher than the required resolution, the difference can be negated within $\approx$ 10 minutes. The positive creep effect must be taken into account when using the DMI in an experimental campaign. The zero creep was found to be negligible. The non-linearity was then recorded using masses between 100 g and 200 g. Calibrated mass against the signal voltage response from the DMI is shown in Fig. 3. The difference between the line of ideal linear response and the measured signal voltage is used to calculate the non-linearity. The non-linearity for this mass range was found to be negligible (0.014 %FS) with detailed results shown in Table 2. The difference between creep response measurement for the 100 g mass and the linear response measurement is due to a change in the zero-offset between experiments. For calculating unknown total masses, it is therefore important to take a zero measurement before the reading is taken. This is not the case for calculating changes in dynamic masses as the zero-offset is negated.

(ii) The results for the sensitivity calibrations are shown in Fig. 4. The percentage error between the calibrated mass and calculated mass is shown against the calibrated mass values. The same data set is shown multiple times with different chosen sensitivities. It is of note the error over this range is small (< 0.1 %). A variable sensitivity, dependent on the signal voltage of the load cell, was also used to calculate the output masses. The difference in accuracy between the variable sensitivity and a optimised constant sensitivity was negligible and therefore a constant sensitivity was selected for simplicity. For the load cell used in this calibration, the optimum sensitivity is estimated to be 0.68875 mV/V as that sensitivity possesses the lowest percentage error in the sample mass range. However, it should be noted that this will be different for different load cells and may change

Table 2. Data of the non-linearity experiments performed with the DMI. Eight calibrated masses were measured on an external mass balance. The DMI was used to measure the signal voltage output from each mass. The percentage error between the signal voltage and line of best fit from Fig. 3 is given to calculate the non-linearity.

Calibrated Mass (g)	Signal Voltage (mV)	Percentage Error (%)
100.0	0.876	-0.10
125.5	1.038	-0.02
130.2	1.068	-0.001
135.1	1.099	-0.007
140.6	1.134	0.01
145.3	1.164	0.03
150.3	1.196	0.07
200.0	1.512	0.13

over time for the same load cell. This indicates regular calibrations are required for the DMI to perform accurately.

(iii) The results for the drift experiment can be seen in Fig. 5. The graph shows both the signal voltage of the DMI and the temperature of the load cell in that time. A clear drift is seen over the 70 hours as the signal voltage drops from 1.023 mV to 1.010 mV which is an equivalent mass drop of 2.05 g. However, the mass drop rate is an average of 0.03 g/hour with a maximum hourly drop of 0.1 g/hour which is appropriate given that all experiments involving lunar simulants in the current microwave setup will be a maximum of two hours. Also shown in Fig. 5 are the periods in which the load cell is released to a 3 mbar vacuum, marked by blue columns in the x-axis. At these points, there is a clear change in the voltage signal as it initially rises and then decreases. The effect of temperature on the DMI can be accounted for during an experimental campaign using the datasheet provided with the load cell where the temperature coefficient is quoted at 0.1 %FS/10°C. A sample placed on the DMI load arm is sufficiently separated from the load cell that the temperature of the sample itself does not impact the load cell performance.

(iv) Fig. 6 shows the results of the hysteresis experiments with a concentration on the results between 50 g and 200 g. There is no de-load data for the 200 g mass as this is the maximum mass placed. Higher masses, particularly those in the sample mass range, have more accurate measurements with percentage errors < 0.2 %. In the higher mass range, the difference between load and de-loading were negligible as were the differences between repeat measurements.

All of the errors assessed during the calibrations experiments are shown in Table 3. These errors are displayed as a percentage of the full scale which is taken as the signal voltage with 500 g on the load cell (3.17 mV). The total error is calculated through propagation as

$$\sigma = \sqrt{L^2 + R^2 + H^2}. \tag{1}$$

The total error ignores drift and creep as both of these phenomena are systematic errors and can therefore be accounted for when analysing results. Taking the total error as a voltage gives a mass error of ± 0.1 g which equals the requirement for accuracy set in Table 1.

4.2 Dynamic Mass Experiment

The dynamic mass experiments were assessed by comparing the mass change from a mass balance and the DMI. The initial and final readings on the external mass balance had values of 99.4 g and 88.8 g respectively, resulting in a mass loss of 10.5 g. The results of
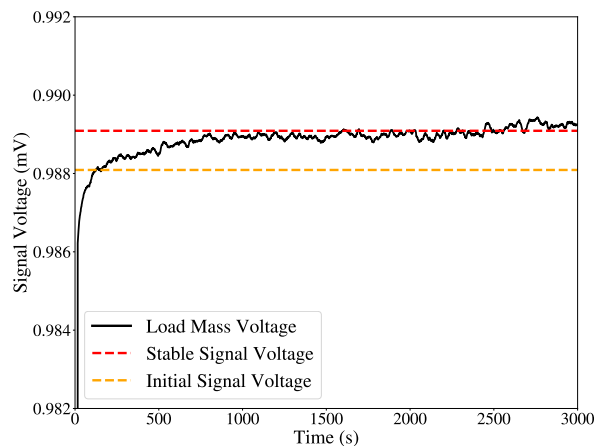

Figure 2. The positive creep observed when loading the DMI with a 100 g calibrated mass. The red dashed line represents the signal voltage when the mass is stable and accurate to the required resolution. The orange dashed line represents the signal voltage upon initial loading. The time difference between the values first being read is 10 minutes.
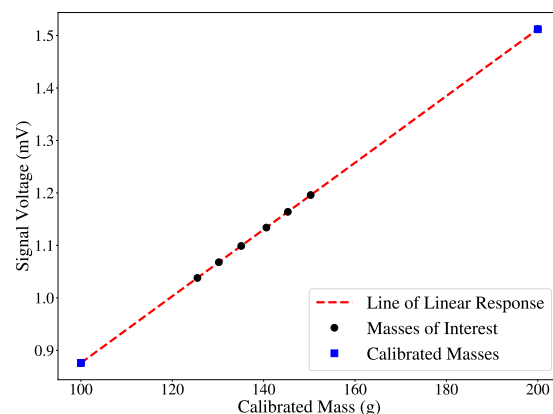

Figure 3. Non-linearity of the DMI between 100 g and 200 g. The signal voltage is displayed against the calibrated masses that were measured on an external mass balance. Blue squares represents the end case masses while black dots represents the masses of highest interest. The red dashed line represents the expected signal voltage values for an ideal linear response.

Table 3. Quantification of the different calibration errors experienced using the DMI. The total error is calculated using Equation 1.

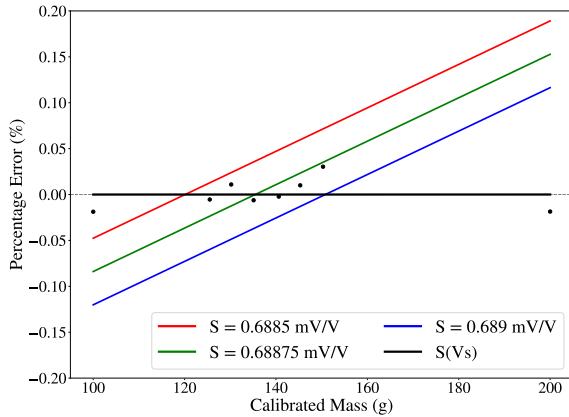| Error	Value
Drift (Vacuum), D	0.020 %FS/Hour
Creep, C	0.030 %FS
Non-linearity, L	0.014 %FS
Repeatability, R	0.012 %FS
Hysteresis, H	0.008 %FS
Total Error, σ	0.020 %FS

Figure 4. A plot of calibrated mass against the percentage error of the mass recorded on the DMI. Various sensitivities are shown to gauge which is more accurate. Also shown is a sensitivity that is a function of the signal voltage (black marker and line).
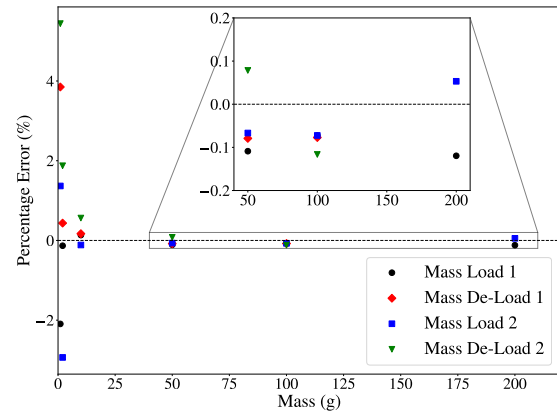

Figure 6. A plot of calibrated mass against the percentage error recorded on the instrument between 1 g and 200 g. The plot gives an indication of both the repeatability and hysteresis of the instrument. The inset shows the percentage error for the 50 g to 200 g section.
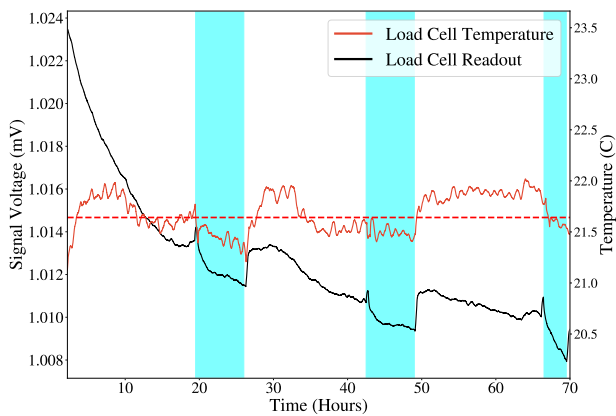

Figure 5. The signal voltage of the DMI left over the course of 70 hours when loaded with a 100 g calibrated mass (black line). Long term drift can be seen along with brief changes in the signal voltage when the load cell is exposed to vacuum (blue regions). Also shown is the temperature of the load cell measured using a K-type thermocouple (red line). The dashed red line represents the mean temperature.

Figure 7. A plot of the recorded mass of a IPA filled crucible in a vacuum environment against time. The grey line shows raw data and the black line shows a rolling average over 30 seconds. The blue point gives the initial mass before the vacuum pump is turned on and the red point gives the final mass before the vacuum pump is turned off. The green dashed line indicates the trend assumed without the use of a DMI, highlighting the DMIs ability to identify previously unseen phenomena.

the mass change calculated from the DMI are shown in Fig. 7. The initial and final masses recorded on the DMI are the same as those measured on the mass balance within ± 0.1 g. This shows that the instrument is able to accurately measure the dynamic mass of a load to within ± 0.1 g in a vacuum environment. The DMI is also able to identify different physical regimes in this experiment. The mass drop in the first 500 seconds is significantly higher compared to the next 3000 seconds where the mass drop rate becomes steady. This implies a high evaporation rate at the start that eventually becomes a steady state loss as the rate of IPA evaporation is matched by the energy required to do so. Such phenomena would not have been identified when measuring the mass before and after the experiment (highlighted in Fig. 7).
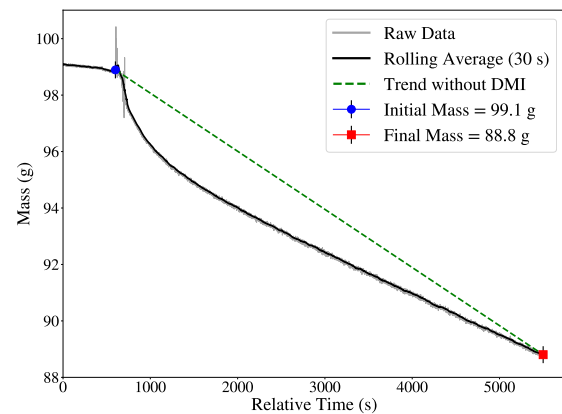
4.3 Microwave Environment Experiment

As can be seen in Fig. 8, the microwave environment experiment shows the mass change for each run over time. As shown in Table 4, the masses measured using the external mass balance and the calculated masses from the DMI are within ± 0.1 g of each other for each separate heating run at each stage of mass measuring. The heating times are different to the total measuring time as additional time was required to get the system down to a pressure of 3 mbar. The results demonstrate the DMI works within the required accuracy for a changing mass in both a vacuum environment and a microwave environment. The 10 minute run loses more mass than the others
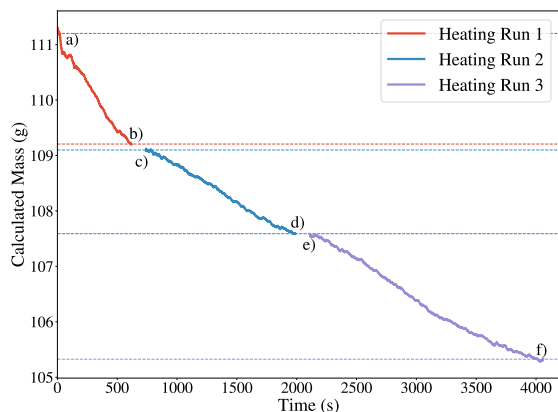
Figure 8. Three separate heating runs of a crucible containing deionised H_2O. Runs were performed for 10, 15, and 30 minutes using 250 W microwaves in a 3 mbar vacuum environment. The heating times are different to the total measuring time as additional time was required to get the system down to a pressure of 3 mbar. a)-f) indicates different mass measuring stages with more detailed in Table 4. The gap between each data set is the time taken to measure the mass on the external mass balance.

Table 4. Results of water mass loss through microwave heating using the DMI. Runs were performed for 10, 15, and 30 minutes using 250 W microwaves in a 3 mbar vacuum environment. The heating times are different to the total measuring time as additional time was required to get the system down to a pressure of 3 mbar. Mass differences calculated using the DMI are shown alongside those measured on a mass balance at each stage to 1 SD.

Run Number	Time (mins)	Stage	V_s (mV)	M_{calc} (g)	M_{meas} (g)
1	10	a)	0.705	111.2 ± 0.1	111.3 ± 0.1
		b)	0.692	109.2 ± 0.1	109.1 ± 0.1
2	15	c)	0.691	109.1 ± 0.1	109.1 ± 0.1
		d)	0.682	107.6 ± 0.1	107.5 ± 0.1
3	30	e)	0.682	107.6 ± 0.1	107.5 ± 0.1
		f)	0.667	105.3 ± 0.1	105.2 ± 0.1

as this experiment was performed with more water mass present in the crucible allowing more efficient heat transfer. As more water is lost, the temperature reduces through the heat of evaporation making subsequent water loss require more energy and hence longer heating times. Temperature readings of the samples could be used to add further evidence to the findings. Unfortunately, the pyrometer in the microwave system could not read the surface temperature of the sample itself due to line of sight issues.

5 DISCUSSION

The DMI is assessed by comparing the performance of the instrument in the calibrations and the experiments to the requirements laid out in Table 1. Calibrations and experiments have confirmed that all the requirements laid out have been met. The DMI has a mass accuracy of ± 0.1 g for masses between 100 g and 200 g in a microwave environment of 250 W and vacuum environment of 3 mbar. For esti-

mating the total mass, a zero offset reading must be taken while for estimating changes in mass, the zero offset reading is not required. Calibrations were not performed at pressures lower than 3 mbar but all components of the DMI are rated to 10^{-5} mbar. The DMI has been successfully designed to be isolated from microwave energy at 250 W and experiences negligible temperature gains due to this. Tests at higher microwave powers are yet to be performed. Samples at 100 K have been placed on the load arm in a vacuum environment with no change in the load signal being experienced suggesting the DMI can operate at the required temperature range (100-400 K). The effect of temperature on the DMI can be accounted for during an experimental campaign using the datasheet provided with the load cell where the temperature coefficient is quoted at 0.1 %FS/10°C and the general effects of temperature on load cell output is well documented (Mattingly et al. 2017). The quoted temperature coefficient is accurate to the signal voltage changes seen in Fig. 5 due to temperature changes experienced when exposed to vacuum conditions. As already seen in Fig. 7, the DMI has been successfully used to identify physical phenomena occurring during an experiment. The rate of mass loss of IPA in a vacuum environment was shown to evolve over time as the mass loss moves from rapid evaporation upon first release to vacuum to a steady state loss regime as the IPA loses energy through evaporation. Without the DMI, the measured mass before and after the experiment would have suggested a different trend losing vital information on the phenomena present. The experiment highlights the DMIs usefulness as an instrument for measuring changing masses to a high precision in a vacuum environment. Improvements to the pyrometer line of sight in the microwave system could be made to measure the surface temperature of evaporating samples. Future work aims to use the DMI in experiments where cryogenic icy lunar simulants are heated up in the microwave cavity using 250 W microwaves in a 3 mbar vacuum environment. Samples will be prepared using a range of water contents and simulants (as done in Cole et al. (2023)), and these samples will be heated up for a suitably long time that all the added water is extracted. By performing the experiments in this manner, the DMI will provide much needed insight into the interaction between microwave energy, lunar simulant and water ice. The DMI will allow the dynamic nature of the interaction to be observed and for conclusions to be drawn about the efficacy of using microwave heating as an ISRU technique for water extraction at the lunar poles. The DMI is a unique instrument as it is not limited for uses in microwave heating experiments, it can be applied to other forms of ISRU where accurate dynamic mass measurements are needed such as using different thermal mining methods or for use in reduction experiments. Changes to the load arm may be required for additional ISRU techniques, e.g. making a load arm that is resilient to temperatures of 900 °C or above. Overall, the DMI has been developed to a stage where it can be used in an experimental campaign of ISRU experiments.

6 CONCLUSIONS

This study describes the development of a Dynamic Mass Instrument (DMI) for use in microwave heating ISRU experiments. A series of calibrations and experiments have been performed to quantify and clarify the behaviour of the instrument in different environments and scenarios. The DMI will allow a greater insight into the interaction of microwave energy, lunar simulant, and water ice. The insights should allow a more thorough quantification of the efficacy and identification of previously unseen phenomena in using microwave heating as a water extraction technique.

ACKNOWLEDGEMENTS

DATA AVAILABILITY

Any data from this work can be made available upon request to the author.

REFERENCES

Anand, M., 2010. Lunar Water: A Brief Review, *Earth, Moon and Planets*, **107**(1), 65–73.

Cannon, K. M. & Britt, D. T., 2020. A geologic model for lunar ice deposits at mining scales, *Icarus*, **347**(May), 113778.

Colaprete, A., Schultz, P. H., Heldmann, J., Wooden, D., Shirley, M., Ennico, K., Hermalyn, B., Marshall, W., Ricco, A., Elphic, R. C., Goldstein, D., Summy, D., Bart, G. D., Asphaug, E., Korycansky, D., Landis, D., & Sollitt, L., 2010. Detection of Water in the LCROSS Ejecta Plume, *Science*, **330**.

Cole, J. D., Lim, S., Sargeant, H. M., Sheridan, S., Anand, M., & Morse, A., 2023. Water extraction from icy lunar simulants using low power microwave heating, *Acta Astronautica*, **209**, 95–103.

Ethridge, E. & Kaukler, W., 2007. Microwave extraction of water from lunar regolith simulant, *AIP Conference Proceedings*, **880**(1), 830–837.

Kornuta, D., Abbud-Madrid, A., Atkinson, J., Barr, J., Barnhard, G., Bienhoff, D., Blair, B., Clark, V., Cyrus, J., DeWitt, B., Dreyer, C., Finger, B., Goff, J., Ho, K., Kelsey, L., Keravala, J., Kutter, B., Metzger, P., Montgomery, L., Morrison, P., Neal, C., Otto, E., Roesler, G., Schier, J., Seifert, B., Sowers, G., Spudis, P., Sundahl, M., Zacny, K., & Zhu, G., 2019. Commercial lunar propellant architecture: A collaborative study of lunar propellant production, *REACH*, **13**, 100026.

Li, S., Lucey, P. G., Milliken, R. E., Hayne, P. O., Fisher, E., Williams, J. P., Hurley, D. M., & Elphic, R. C., 2018. Direct evidence of surface exposed water ice in the lunar polar regions, *Proceedings of the National Academy of Sciences of the United States of America*, **115**(36), 8907–8912.

Lim, S., Bowen, J., Degli-Alessandrini, G., Anand, M., Cowley, A., & Levin Prabhu, V., 2021. Investigating the microwave heating behaviour of lunar soil simulant JSC-1A at different input powers, *Scientific Reports*, **11**(1), 2133.

Lim, S., Degli-Alessandrini, G., Bowen, J., Anand, M., & Cowley, A., 2023. The microstructure and mechanical properties of microwave-heated lunar simulants at different input powers under vacuum, *Scientific Reports*, **13**(1), 1804.

Mattingly, G., Garner, J. & Whitaker, M., 2017. Observed temperature effects on load cells, Tech. rep., Department of Energy.

Metzger, P. T., 2023. Economics of in-space industry and competitiveness of lunar-derived rocket propellant, *Acta Astronautica*.

Paige, D. A., Siegler, M. A., Zhang, J. A., Hayne, P. O., Foote, E. J., Bennett, K. A., Vasavada, A. R., Greenhagen, B. T., Schofield, J. T., McCleese, D. J., Foote, M. C., DeJong, E., Bills, B. G., Hartford, W., Murray, B. C., Allen, C. C., Snook, K., Soderblom, L. A., Calcutt, S., Taylor, F. W., Bowles, N. E., Bandfield, J. L., Elphic, R., Ghent, R., Glotch, T. D., Wyatt, M. B., & Lucey, P. G., 2010. Diviner lunar radiometer observations of cold traps in the moon's south polar region.

Sanders, G. B. & Larson, W. E., 2013. Progress made in lunar in situ resource utilization under NASA's exploration technology and development program, *Journal of Aerospace Engineering*, **26**(1), 5–17.

Schlüter, L. & Cowley, A., 2020. Review of techniques for In-Situ oxygen extraction on the moon, *Planetary and Space Science*, **181**, 104753.

Taylor, L. A. & Meek, T. T., 2005. Microwave Sintering of Lunar Soil: Properties, Theory, and Practice, *Journal of Aerospace Engineering*, **18**(3), 188–196.

Watson, K., Murray, B., & Brown, H., 1961. On the Possible Presence of Ice on the Moon, *Journal of Geophysical Research*, **66**(5).

Yaw, K. C., 2012. Measurement of dielectric material properties, Tech. rep., Application Note. Rhode & Schwarz.